Title
Powerful, pulsed, THz radiation from laser accelerated relativistic electron bunches

Authors
Toth, Cs
Tilborg, J. van
Geddes, C.G.R.
et al.

Publication Date
2004

Powerful, pulsed, THz radiation from laser accelerated relativistic electron bunches

Cs. Tóth[a], J. van Tilborg[a,b], C. G. R. Geddes[a,c], G. Fubiani[a,d], C. B. Schroeder[a], E. Esarey[a], J. Faure[e] G. Dugan[f], and W. P. Leemans[a]

[a]Lawrence Berkeley National Laboratory, 1 Cyclotron Road, Berkeley, CA 94720, USA;
[b]also at Technische Universiteit Eindhoven, the Netherlands;
[c]also at University of California, Berkeley, CA, USA;
[d]also at Université de Paris XI, Orsay, France;
[e]presently at Laboratoire d'Optique Appliquée, Paris, France;
[f]Cornell University, Ithaca, NY 14853, USA

ABSTRACT

Coherent THz radiation was produced from relativistic electron bunches of subpicosecond duration. The electron beam was produced by strongly focused (≈ 6 μm), high peak power (up to 10 TW), ultra-short (≥ 50 fs) laser pulses of a 10 Hz repetition rate Ti:sapphire chirped pulse amplification (CPA) laser system via self-modulated laser wakefield acceleration (SM-LWFA) in a high density ($> 10^{19}$ cm^{-3}) pulsed gas jet. As the electrons exit the plasma, coherent transition radiation is generated at the plasma-vacuum boundary for wavelengths long compared to the bunch length. Radiation yield in the 0.3 to 19 THz range and at 94 GHz has been measured and found to depend quadratically on the bunch charge. The measured total radiated energy in the THz range for two different collection angles is in good agreement with theory. Modeling indicates that optimization of this table-top source could provide more than 100 μJ/pulse. Together with intrinsic synchronization to the laser pulse, this will enable numerous applications requiring intense terahertz radiation. This radiation can also be applied as a useful tool for measuring the properties of laser accelerated bunches at the exit of the plasma accelerator.

Keywords: ultrahigh-fields, ultra-short, laser-plasma, wakefield, electron-acceleration, THz-emission, transition radiation

1. INTRODUCTION

Terahertz radiation is non-ionizing electromagnetic radiation with sub-millimeter wavelength, which can be used to non-invasively measure optical properties of materials with hundred micron resolution. Terahertz radiation have applications[1,2] in biological imaging, material screening, semi-conductor imaging, surface chemistry, and high-field condensed matter studies. High peak power radiation is required for rapid two-dimensional imaging[3] and for non-equilibrium and non-linear studies that require MV/cm fields.[2] Laser-triggered solid-state based sources of THz radiation have been developed that rely on switched photoconducting antennas (e.g., see Weling *et al.*[4] and references therein) or optical rectification of femtosecond pulse trains.[5] Large aperture biased GaAs structures, operated at 1 kHz repetition rate, have produced on the order of 0.5 μJ/pulse.[6] Most other sources using either laser switched structures or optical rectification have operated at high frequency (10's of MHz) with μW–mW level average power.

Alternatively, far infrared and THz radiation can be generated from electron beams (e-beams) through various methods, including bending in a magnetic field (synchrotron radiation)[7] and by traversing a medium with a discontinuity in dielectric properties (transition radiation).[8–10] The radiation is coherent when electrons in a bunch emit in phase, that requires the bunch structure be shorter than the radiation wavelength λ. The coherent

Send correspondence to Cs.T or W.P.L.
Cs. T.: E-mail: CToth@lbl.gov, Telephone: 1 510 486 5338
W.P.L.: E-mail: WPLeemans@lbl.gov, Telephone: 1 510 486 7788

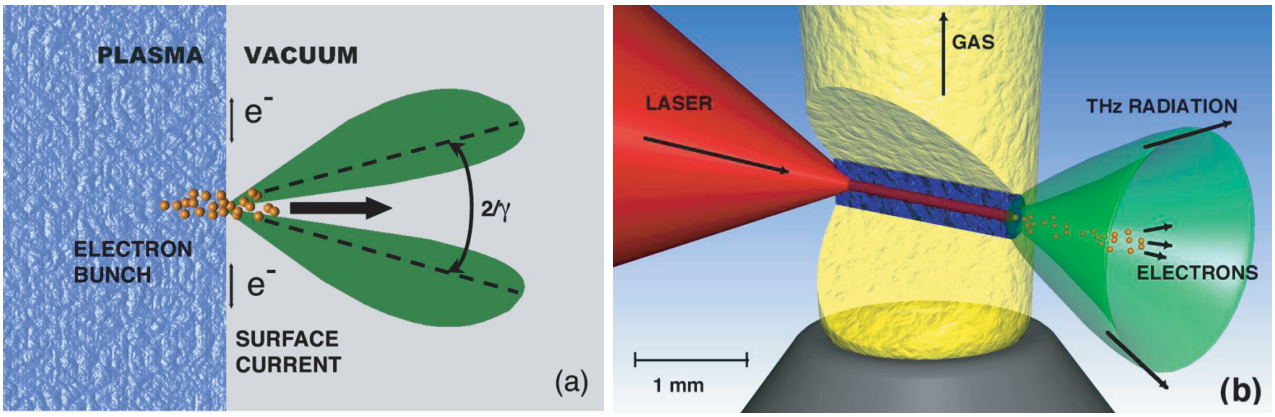

Figure 1. (a) Schematic of transition radiation production by an electron beam crossing the plasma-vacuum boundary. Surface currents are excited at the boundary and generate radiation which peaks at a half angle on the order of $1/\gamma$. (b) Schematic of interaction region showing a multi-terawatt laser beam (red cone on the left) focused onto a high density gas jet plume (yellow column in the center) that emerges from a supersonic gas nozzle (grey on the bottom). When the laser enters the gas plume, it rapidly ionizes the gas (blue region), self-channels through the plasma and generates a beam of relativistic electrons (golden dots). When the electrons propagate through the plasma-vacuum boundary, coherent THz radiation is generated in a cone-like angular distribution (green cone on the right). Part of the gas plume cut out on the picture to reveal the details of the ionized inner regions of the plasma.

radiation intensity scales quadratically with the total charge, rather than linearly as in the case of incoherent emission. Conventional accelerators can produce sub-ps bunches containing pC's of charge,[11,12] operating at high repetition rate and hence generating high average THz radiation power.[13] They also provide a solution for producing THz emission with a narrow divergence angle, given by $1/\gamma$, where $\gamma = 1/\sqrt{1-(v/c)^2}$ is the relativistic Lorentz factor, v the electron velocity, and c the speed of light. However, bunch lengthening and emittance growth due to space charge effects limit the charge per bunch in these short bunches to pC's and, hence, limit the radiated peak power. The 0.5 μJ/pulse produced by the linac-based source,[13] as well as present solid state THz radiation sources[6] (limited by material damage), is insufficient for high field applications that require multi-MeV/cm. Achieving high pulse energy is therefore an important challenge that will enable numerous applications requiring intense THz beams.

Recently Leemans *et al.*[10] demonstrated, that coherent THz radiation can be produced from laser accelerated electron bunches. In this paper we present experimental details on this electron beam based THz source that has the potential to achieve unprecedented levels of energy (up to tens of mJ per pulse, several orders of magnitude beyond that of conventional THz radiation sources) and that relies on two novel components: (1) extremely dense, sub-ps electron bunches produced with a table-top laser-plasma-based accelerator and (2) the production of coherent transition radiation at the boundary between a plasma and vacuum.[10,14] Laser wakefield accelerators (LWFA, to be described in detail in Sec. 4) rely on the excitation of large amplitude longitudinal plasma waves with an intense laser and can operate with 1–100 GV/m accelerating gradients. These large fields can accelerate more than 10^{10} background electrons to relativistic energies,[15,16] albeit with 100% energy spread. They can produce ultra-short (femtosecond) bunches containing nC's of charge because space charge effects are mitigated inside the accelerator structure through shielding provided by the background ions in the plasma. This is not the case in a conventional accelerator and limits the achievable peak current in those accelerators. To produce high peak power coherent radiation, emission must occur before space charge and energy spread effects cause bunch density reduction during propagation in vacuum. This requirement is naturally satisfied by generation of transition radiation at the plasma-vacuum boundary of the LWFA, provided certain criteria regarding transverse size and longitudinal gradient are satisfied. Terahertz emission from laser excited plasmas had been reported earlier[17] and was attributed to the excitation of radial plasma density oscillations at a plasma density resonant with the laser pulse duration. This mechanism predicts very low emission at densities used in our experiments and does not rely on production of accelerated electrons. In addition, the far-field radiation pattern shows no emission

in the forward (laser) direction. Evidence for incoherent transition radiation has been observed in the optical regime from fast electron generation in laser interactions with solid targets.[18] Coherent transition radiation at longer wavelengths could potentially be generated in laser-solid target experiments from the interaction of the fast electrons with the rear-side of the solid target.

The structure of this paper follows the key elements of the laser-plasma interaction and the THz generation process as depicted in Fig. 1. The theory of generation of transition radiation from a relativistic electron bunch crossing a plasma-vacuum boundary (Fig. 1(a)) will be summarized in Sec. 2. Section 3 describes the Ti:sapphire chirped pulse amplification (CPA) multi-terawatt, multi-beam laser system specifically designed for laser-plasma acceleration studies at the L'OASIS Lab of LBNL. One arm of this laser system provides the final focused optical beam, shown as an incoming cone of optical radiation on the left side of Fig. 1(b). The mechanism of the relativistic electron beam generation (center part of Fig. 1(b)) via self-modulated laser wakefield acceleration is the subject of Section 4. The next part of the paper, Sec. 5, discusses the measurement details of the THz radiation (on the right in Fig. 1(b)) emanating from the interaction region and presents evidence for the coherent nature of the radiation in the 0.3 to 19 THz range, polarization measurements, and frequency spectrum measurements. Using these spectral measurements, electron bunch durations on the order of 30-50 fs are inferred based on comparison to theoretical spectrum calculations. Section 6 summarizes the results and discusses ways of increasing the radiated energy beyond what has been achieved in the present experiments.

2. THEORY OF TERAHERTZ EMISSION FROM PLASMA BOUNDARY

Modelling of the radiation process can be done by assuming that the plasma (with dielectric constant $\epsilon = 1 - \omega_p^2/\omega^2$, where ω_p and ω are the plasma and radiation frequencies, respectively) is equivalent to a conductor with a sharp conductor-vacuum boundary. The transition radiation will be generated by electron beam induced polarization currents at plasma densities below the critical density (where $\omega_p = \omega$) for the radiation wavelength. The plasma density profile used in the experiments had a sufficiently large gradient such that the dielectric constant satisfied $|\epsilon| \gg 1$ within a distance of the order of a skin depth, and therefore the plasma can be well-modeled as a conductor for frequencies $\omega < \omega_p$. In addition, provided the plasma scale length is short compared to the radiation formation length, then the dielectric interface radiates as if it were a sharp dielectric-vacuum boundary.

With these assumptions, the energy radiated, per unit frequency $d\omega$ and per unit solid angle $d\Omega$, from a single electron traversing the dielectric boundary is given by the well-known result[8, 9, 19]

$$\frac{d^2W_e}{d\omega d\Omega} = \left(\frac{r_e m_e c}{\pi^2}\right) \frac{u^2\left(1+u^2\right)\sin^2\theta}{\left(1+u^2\sin^2\theta\right)^2}\,, \tag{1}$$

where θ is the observation angle with respect to the electron trajectory (assumed to be normal to the plasma surface and along the z-axis), $u = \gamma v/c$ is the electron momentum normalized to $m_e c$, c is the speed of light, m_e is the electron rest mass, and $r_e = e^2/m_e c^2$ is the classical electron radius. The radiation pattern is zero along the axis ($\theta = 0$) and peaks at a radiation cone angle of $\theta \sim 1/\gamma$ (assuming $\gamma \gg 1$). The differential energy radiated by a single electron $d^2W_e/d\omega d\Omega$ is independent of frequency. In practice, however, the maximum wavelength radiated will be limited, for example, by the physical dimensions of the system (e.g., the transverse plasma boundary). Integrating Eq. (1) over solid angle yields $dW_e/d\omega \simeq (2/\pi) r_e m_e c \ln(\gamma)$, in the highly-relativistic limit $\gamma \gg 1$. The radiation from the beam of electrons sums incoherently for wavelengths short compared to the bunch length, i.e., $W_{\rm ITR} \simeq N W_e$, where N is the number of electrons in the bunch, and a monoenergetic divergenceless beam was assumed. For wavelengths long compared to the bunch length, the radiation sums coherently, i.e., $W_{\rm CTR} \simeq N^2 W_e$. In particular, the total coherent radiated energy over all angles and frequencies is given by $W_{\rm tot} \simeq \left(4 r_e m_e c^2\right) N^2 \ln(\gamma)/\lambda_{\rm min}$, assuming $\gamma \gg 1$, where $\lambda_{\rm min}$ is the minimum wavelength for which the bunch radiates coherently and is determined by the electron bunch dimensions (i.e., coherence effects). The total coherent energy can be written in practical units as $W_{\rm tot}[\mathrm{J}] \simeq 3.6 \times 10^{-2} (Q[\mathrm{nC}])^2 \ln(\gamma)/\lambda_{\rm min}[\mu\mathrm{m}]$, where Q is the bunch charge. For example, Q = 5 nC ($N = 3.1 \times 10^{10}$), $\gamma = 10$, and $\lambda_{\rm min} = 200$ μm give $W_{\rm tot} \simeq 10$ mJ, which is several orders of magnitude beyond that of conventional sources.

The above analysis can be generalized for the case of an arbitrary electron beam momentum distribution. Assuming full coherence, and for the case of a divergenceless beam with normalized energy distribution $g(u)$, the differential energy spectrum of the coherent transition radiation is

$$\frac{d^2W_{\rm CTR}}{d\omega d\Omega} = \left(\frac{r_e m_e c}{\pi^2}\right) N(N-1)\sin^2\theta \left| \int du g(u) \frac{u\left(1+u^2\right)^{1/2}}{1+u^2\sin^2\theta} \right|^2 . \quad (2)$$

Using Eq. (2), the total coherent radiation energy into a small collection angle $\theta \leq \theta_{\rm coll} < 1/\langle u\rangle$, and for a bandwidth $\Delta\omega/\omega$ is

$$W_{\rm CTR} \simeq m_e c^2 (r_e/\lambda) N(N-1)(\Delta\omega/\omega)\theta_{\rm coll}^4 \langle u^2\rangle^2 , \quad (3)$$

assuming $\langle u^2\rangle > 1$, where the brackets indicate an average over the momentum distribution. Laser-plasma generated electron beams in the self-modulated regime can be characterized by a Boltzmann momentum distribution $g(u) = u_{\rm T}^{-1}\exp[-u/u_{\rm T}]$, where $u_{\rm T}$ is the temperature of the distribution. The amount of radiated energy in the collection cone half-angle $\theta_{\rm coll} < 1/u_{\rm T} < 1$ and frequency bandwidth $\Delta\omega/\omega$ is given by $\Delta W_e \simeq 4m_e c^2 (r_e/\lambda) N^2 (u_{\rm T}\theta_{\rm coll})^4 (\Delta\omega/\omega)$. For example, $\Delta W_e = 30$ μJ within $\theta_{\rm coll} = 50$ mrad for a 1.5 nC bunch with temperature $u_{\rm T} = 9$ in a bandwidth 0.3 to 3 THz. Due to the strong dependence on electron energy and angle, $W_{\rm CTR} \propto (\gamma\theta_{\rm coll})^4$, the measured energy can easily be increased by increasing either the electron energy γ or the cone angle $\theta_{\rm coll}$ of the collection optics (for $\theta_{\rm coll} < 1/\langle u\rangle$).

The spectrum of the radiation and total energy radiated will be strongly influenced by the effects of coherence and the transverse size of the dielectric structure (i.e., by diffraction from the plasma edge). Coherence effects will set the minimum wavelength radiated to the size of the electron bunch structure. For a Gaussian bunch, coherent radiation requires $2\pi\sigma_z < \lambda$, where σ_z is the rms bunch length. Schroeder *et al.*[14] calculated the influence of diffraction from the transverse edge of the plasma to the coherent transition radiation generated at a plasma-vacuum interface. The finite transverse extent of the plasma produces a wavelength dependence in the differential energy for fully-coherent radiation and strongly modifies the spectrum for $\rho \sim \gamma\lambda$, where ρ is the characteristic transverse size of the plasma. (i.e., the spectrum is influenced by diffraction effects when the transverse size of the plasma ρ is of order the transverse extent of the self-fields of the relativistic electrons $\sim \gamma\lambda$). Distortion of the spectra increases with larger energy, and the spectra are suppressed for decreasing transverse size. In general, the spectral region of coherent radiation is approximately $2\pi\sigma_z < \lambda < 2\pi\rho/u$, where the lower bound is due to longitudinal coherence and the upper bound is due to diffraction effects.

3. THE LASER: A MULTI-TERAWATT, MULTI-BEAM TI:SAPPHIRE SYSTEM

Complex laser-plasma interaction studies, such as development of laser wakefield accelerators,[16,20–22] X-ray lasers, and laser fusion research require synchronized, multiple beams of high intensity light pulses. In most cases, it is also desirable that these beams have different pulse durations, wavelengths, and pulse energies for various stages of plasma preparation, excitation, and diagnostics. We describe here the L'OASIS (Lasers, Optical Accelerator Systems Integrated Studies) Laser Facility of the Lawrence Berkeley National Laboratory (LBNL), Berkeley, CA, a facility that has been specially designed for studying high field laser-plasma interactions and particularly aimed for the investigations of laser wakefield particle (electron, protons, ions) acceleration (Fig. 2). The core of the 10 Hz chirped pulse amplification (CPA), Ti:sapphire (800 nm) laser system is a Kerr-lens mode-locked master oscillator (Femtolasers). After an acousto-optic spectral phase compensating device (FastLite "Dazzler") the pulses are lengthened to 220 ps in a grating based optical stretcher. The stretched pulses are amplified in a regenerative amplifier (Positive Light "Spitfire") to 1.2 mJ energy. About 20% of this output energy is compressed here and subsequently frequency doubled in a nonlinear crystal (β-Barium-Borate, BBO) for plasma diagnostic purposes. The remainder (80%) is amplified to 33 mJ in a 3-pass 'pre-amplifier'. At this point the beam is split towards three independent Ti:sapphire power amplifiers, each pumped by frequency doubled Nd:YAG lasers (Spectra Physics "GCR 350-PRO" and Positive Light custom system). The beam energy of the first power amplifier reaches 1 J after 5 passes in the 28 mm diameter, 25 mm long Ti:sapphire crystal. This beam is then transported through an evacuated beam pipe into vacuum chambers containing optical compressors in a radiation-shielded target cave for compression and for experiments.

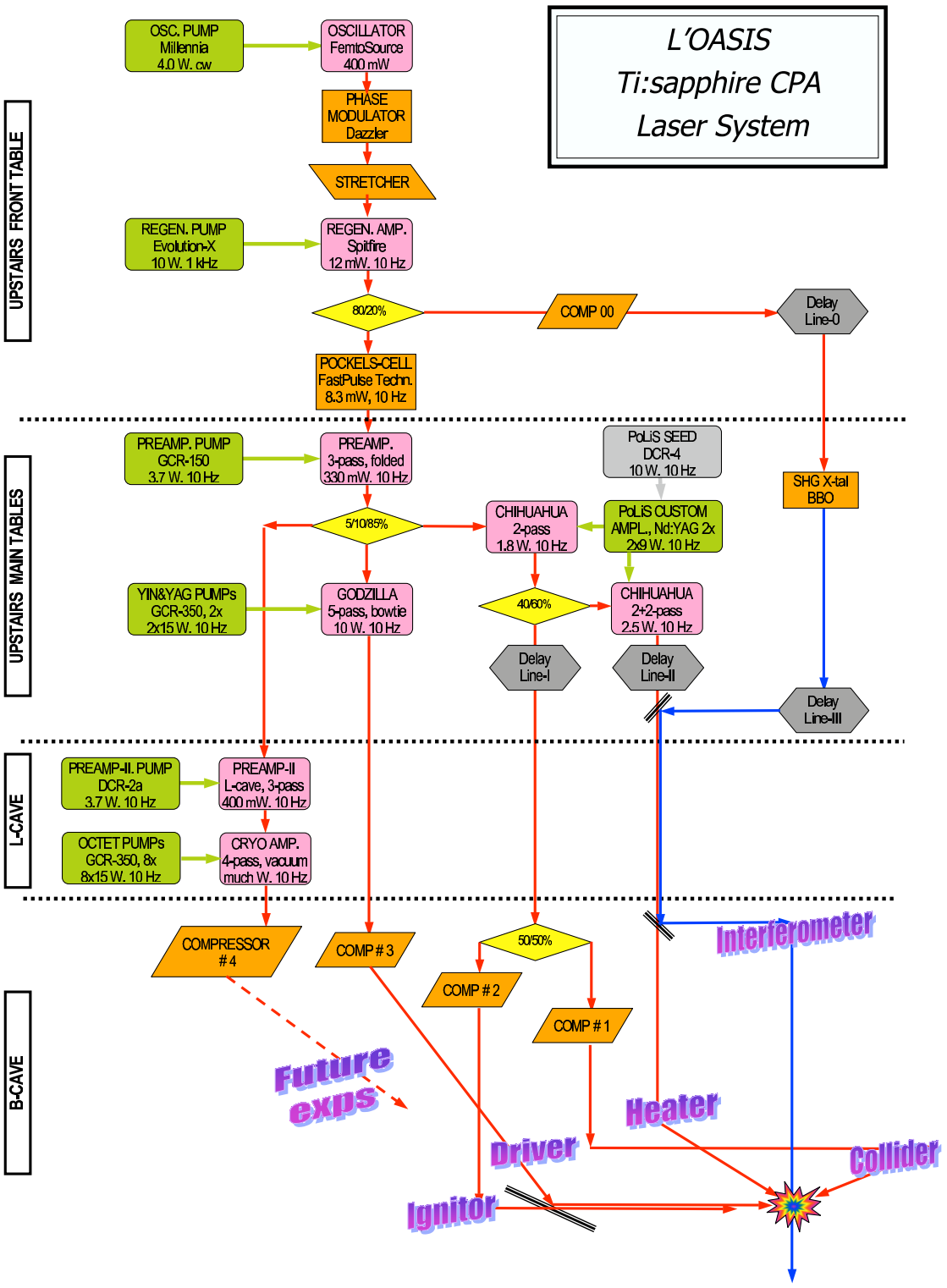

Figure 2. Flowchart of the L'OASIS (Lasers, Optical Accelerator Systems Integrated Studies) Laser Facility, a highly automated and remote controlled, multi-beam, multi-terawatt, Ti:sapphire CPA laser system. It provides synchronized beams of 2x1.0-TW, 12-TW, and 100-TW peak-power in a unique, radiation shielded environment, specially designed to study laser wakefield acceleration of charged particles in plasmas.

Table 1. Laser beam parameters and purpose of each beam in the current laser wakefield accelerator setup of the L'OASIS Laboratory of LBNL.

	Purpose	Energy/Pulse	Pulse length	Peak power	Average power
Main Amp	Wakefield Driver	550 mJ	46 fs	12 TW	5.5 W
Secondary Amp	Collider Beam	50 mJ	50 fs	1 TW	0.5 W
Secondary Amp	Plasma Ignitor	50 mJ	50 fs	1 TW	0.5 W
Secondary Amp	Plasma Heater	250 mJ	220 ps	1.1 GW	2.5 W
Regen. Amp	Interferometry	30 μJ	50 fs	0.6 GW	0.3 mW
Cryo Amp	Future exps.	3.5 J	35 fs	100 TW	35 W

The second power amplifier's beam is partially dumped after the second pass, resulting a 180 mJ (partial 2nd pass) output and a 250 mJ (2+2 pass final) output energy beams. The former output is split again (collider and ignitor beams) for separate compressions in the target chamber, and the latter one is kept uncompressed, serving as a heater beam in plasma channel experiments.[21] The third power amplifier is currently being commissioned and aims at producing 100 TW (3.5 J/pulse in 35 fs pulses) at 10 Hz repetition rate. This laser uses the third portion (1 mJ) of the preamplifier output as a seed for another 3-pass amplifier followed by a cryogenically cooled, 4-pass amplifier (40 mm diameter, 30 mm long Ti:sapphire crystal), fully enclosed in a vacuum chamber. The amplified beam is propagated in vacuum tubes to the radiation shielded experimental area for final compression. The amplifier system is characterized and continuously monitored via local area network (LAN) from a radiation shielded control room by an array of diagnostics, including beam profile monitoring cameras, remote controlled alignment options, beam-pointing stabilization loops, and pulse measurement tools, such as single-shot autocorrelator (SSA) for pulse duration and third-order correlator (TOC) for contrast measurements. Frequency resolved optical gating (FROG) was used for pulse shape studies.[23] In addition to the flowchart of the system shown in Fig. 2, the main parameters of the the various beam paths are summarized in Table 1.

4. THE RELATIVISTIC ELECTRON BEAM

4.1. Laser Wakefield Acceleration (LWFA) of Electrons

Laser-driven, plasma-based accelerators[24] hold the potential of becoming compact alternatives to conventional radio-frequency-based linear accelerators (linacs). Accelerating gradients in the 10's to 100's GV/m have been measured in laser wakefield accelerator (LWFA) experiments,[15, 16, 25–29] which is three orders of magnitude higher than in conventional linacs. Acceleration of electron bunches containing several nC of charge and energy spectra characterized by a Boltzmann-like distribution with an equivalent temperature ranging from the few MeV to tens of MeV has been demonstrated in the self-modulated regime of the LWFA.[27–29] Recently, experiments have measured electrons with energies above 200 MeV.[15, 30] Although the use of laser-plasma accelerators for high energy physics applications will require performance well beyond todays achievements, several applications with less stringent beam property requirements are becoming possible. One of these is radio-isotope production through (γ, n) reactions with laser accelerated bunches,[22, 31] which requires a sufficient number of electrons with energy in excess of 10's of MeV, a condition that is relatively straightforward to obtain using laser-plasma-based accelerators.

4.2. Laser Wakefield Accelerator Set-up

The LWFA experiments reported here used the 10 TW arm of the laser system described in Sec. 3. The 'Main Amplifier' output reached 1 J/pulse level, and then compressed using a grating based optical compressor. Following compression, the laser beam was focused to a spot size $w = 6$ μm with a 30 cm focal length (f/4) off-axis parabola onto a pulsed gas jet. The peak power P of the laser was varied using both the pulse duration and laser energy. In the THz experiments presented here, the peak power of the pulses at optimum compression [55 fs full-width-half-maximum (FWHM) duration] was $P \simeq 8.3$ TW, resulting in a calculated peak intensity

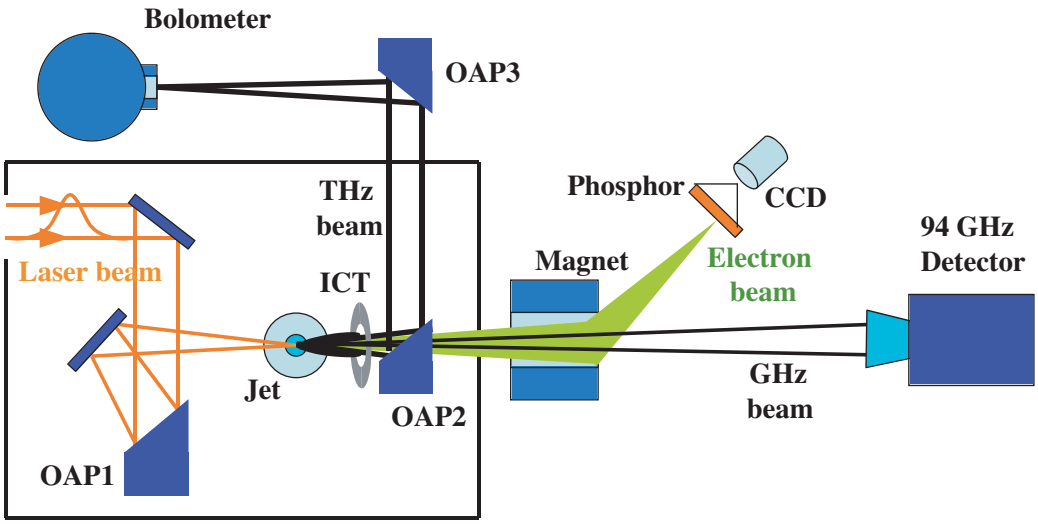

Figure 3. Schematic of the experimental set-up. The high power laser beam is focused using an off-axis parabolic mirror (OAP1) onto a high pressure pulsed gas jet operating with about 70 bar He backing pressure. An integrating current transformer (ICT) is used to measure the charge per bunch of the electron beam produced in the laser ionized gas jet. A double focusing magnetic spectrometer is used to measure the electron beam energy by scanning the magnet excitation current. Radiation is collected with the use of another off-axis parabola (OAP2) with a hole in the middle to transmit the high power laser beam and electron beam. OAP2 collimates the radiation which is transmitted through a silicon window and then focused using OAP3 onto the bolometer. This optical system collects radiation with angular direction between 80 mrad and 300 mrad. The measurements of the radiated energy in a 30 mrad solid angle were done in a separate set-up by focusing the radiation onto the bolometer using a single metal coated spherical mirror with a 50 cm focal length, located about 1 m away.

$I = 2P/\pi r_s^2 \simeq 1.5 \times 10^{19}$ W/cm^2 and a normalized laser strength $a_0 \simeq 8.6 \times 10^{-10} \lambda[\mu\text{m}] I^{1/2}[\text{W/cm}^2] \simeq 2.6$. The gas jet was backed with up to 70 bar helium gas. The profile of the jet had a 1.8 mm flat top at a density of about 3×10^{19} cm^{-3} with a ramp of 1 mm length to zero density on either side (a total length of just under 4 mm). The plasma density profile, measured with a folded-wave interferometer using 400 nm wavelength, 50 fs duration laser pulses, had a typical transverse size of 100 μm $\pm$ 15 μm. The layout of the 'THz-LWFA' experiments is shown in Fig. 3, detailing the final vacuum chamber with the relevant diagnostic components.

4.3. Measurements of the Electron Beam Properties

The charge per bunch and electron beam spatial profile were measured using an integrating current transformer (ICT) and a phosphor screen (retractable from the beam path, not shown in Fig. 3) located 50 cm and 75 cm away from the exit of the gas jet, respectively. The response of the phosphor screen (number of counts on the CCD vs. deposited charge) was calibrated against the ICT. The energy distribution was obtained using an imaging magnetic spectrometer[32] and a phosphor screen with CCD camera. At a given excitation current of the magnet, the momentum acceptance of the magnetic spectrometer was $\delta p/p = \pm 2\%$. A spectrum ranging from 0-50 MeV was obtained by recording the total light yield on the CCD image (corrected for background counts) for excitation currents ranging from 0 to 45 A.

A typical energy spectrum is shown in Fig. 4 and is reasonably well approximated by a Boltzmann distribution with a temperature of 4.6 MeV. The electron beam profile was found to be dependent on laser power. Two representative electron beam images are shown in Fig. 5. The beam divergence was found to be in the range of tens of mrad. For power levels near the maximum power, electron beams were observed with a divergence less than 10 mrad (FWHM) [see Fig. 5(b)]. The amount of charge contained in the small beams was typically about 5% of the large beam and ranged between 30–50 pC. The energy of this part of the beam was not measured separately. However, the shot-to-shot fluctuation in beam divergence near maximum power was found to be

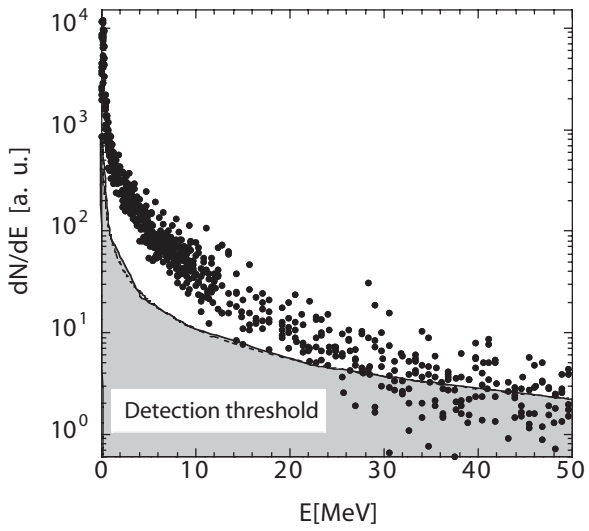

Figure 4. Electron energy spectrum measured using a double focusing imaging magnetic spectrometer. The spectrum was obtained by scanning the current of the magnet and measuring the intensity of the light induced by the electrons hitting a phosphor screen. For any given current, the momentum acceptance $\delta p/p$ of the spectrometer was $\pm 2\%$. Each data point represents 10 shots. The spectrum is reasonably well approximated by a Boltzmann distribution with an effective temperature of 4.6 MeV.

significantly larger than for the lower power cases. In addition, the pointing varied from shot-to-shot by more than 20 mrad. For power levels which exceed the critical power for self-focusing by a factor of 5 or more, the laser self-channeling and particle trapping processes operate in a highly non-linear regime, which likely results in a loss of reproducibility due to sensitivity to operating parameters. In addition, pre-pulse effects have been shown to be important in the acceleration process and the production of stable beams.[33]

Assuming that the electron beam originated from a spot size equal to the laser spot size w, a value for an unnormalized rms geometric "emittance" for the high power case can be estimated to be 0.01 mm mrad, by simply multiplying the assumed source size and measured divergence angle. Similarly low "emittance" values between 0.01 and 0.1 π mm mrad have been reported previously.[33,34] However, there are many reasons why the assumption that the electron beam size is equal to the laser spot size underestimates the actual beam emittance. Prior to interpreting these measurements into electron beam emittance values, as commonly used for conventional accelerators, a thorough understanding of all phase space properties of the beam is required, including energy (mean and spread) and bunch length, as a function of propagation distance. Upon exiting the plasma, the high density electron bunch is subjected to significant space charge forces that can result in transverse beam blow-up as well as modifications to the longitudinal bunch shape and energy distribution. In general, longitudinal space charge forces are expected to lengthen the bunch, thereby reducing the density and, consequently, the effect of transverse space charge forces while the beam is propagating through vacuum.[35,36] Also, the large energy spread can result in ballistic spreading of the electron bunches since fast electrons would outrun the slower ones. More complicated modifications of the energy distribution and correlations in momentum and physical space can still occur however, complicating the interpretation of the data. As an example, if the bunch initially has slow electrons in the front and back, and fast electrons in the middle, bunch compression can occur during the propagation resulting in a temporary increase in space charge forces. More detailed measurements of the energy (mean and spread), bunch length and transverse characteristics of these low divergence beams are needed to fully understand their behavior during propagation in vacuum, and to properly assign an emittance value. Pepper pot based measurements of electrons that were energy filtered around 55 MeV have recently been carried out[37] in a LWFA setup similar to ours and indicate a normalized emittance of 3 π mm mrad at the spectrometer location.

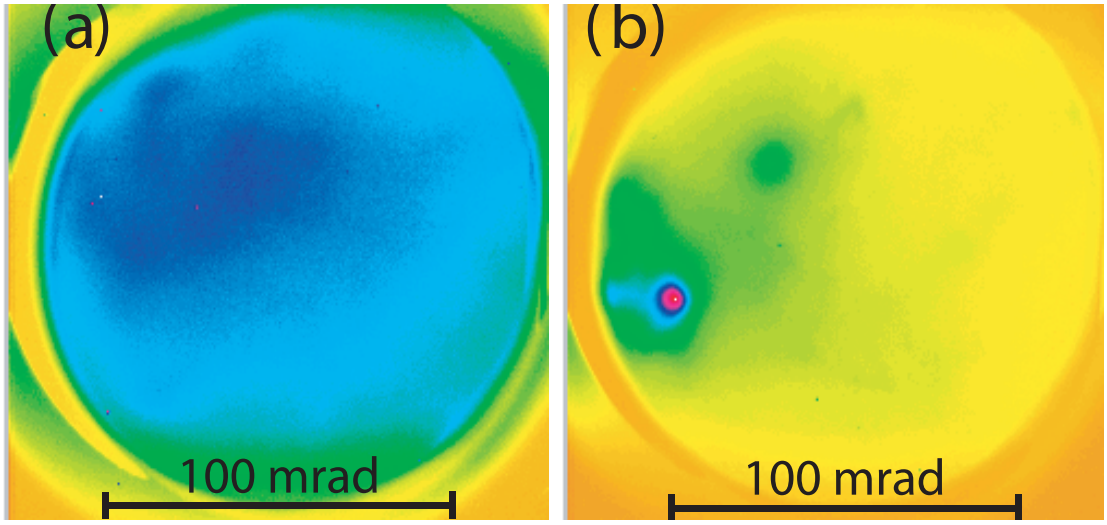

Figure 5. Electron beam images measured by imaging a 10 cm diameter phosphor screen located 75 cm away from the gas jet with a CCD camera, for laser peak power (a) around 2-4 TW and (b) around 8 TW. The unnormalized geometric rms "emittance" for the small spot is 0.01 mm-mrad, obtained by multiplying the assumed source size from which the beam originates (6 μm FWHM, i.e., equal to the laser spot size) and a 10 mrad (FWHM) divergence angle.

5. TERAHERTZ RADIATION MEASUREMENTS

The radiation measurements were done in two different frequency ranges: at 94 GHz using a mm-wave heterodyne detection system and from 0.3–19 THz using a liquid helium cooled bolometer. The details of the 94 GHz measurements are reported elsewhere,[38] here we focus on the THz range measurements only.

5.1. Radiation Collection Geometries

To verify the dependence of radiated energy on collection angle, two different set-ups were used in the THz frequency range. In the first set-up, with a collection angle of 30 mrad, radiation was reflected out of the vacuum chamber through a window using a 5 μm thick metal coated nitrocellulose foil 30 cm from the gas jet. (Although transition radiation will be generated when the beam propagates through this foil, the emission is incoherent due to bunch lengthening[36] and transverse beam size increase at that location, measured with a phosphor screen.) The radiation then propagated in air and through laser beam attenuators, and was focused with an f/30 metal coated spherical mirror onto a cooled (4.2 K) Si-based bolometer, equipped with an internal 3 THz low-pass filter, to measure the radiated energy.

To improve the collection efficiency, the second set-up used an off-axis 90° parabola (effective focal length of 127 mm) to collimate THz light onto a second off-axis parabola (effective focal length of 177.8 mm). After exiting the vacuum chamber through a silicon window, the radiation was incident on the bolometer which was positioned in the calculated focal position. Note that a hole was drilled on axis through the first parabola to allow the 800 nm laser beam to propagate through the parabola, resulting in a collection angle (half-cone) covering emission angles between $80 < \theta < 300$ mrad. The complete bolometer system sensitivity (Volts per incident energy) including a gain factor of the internal amplifier of 1000 and the bolometer internal collection efficiency was calibrated and found to be 1 V of signal per 4.0 pJ of incident THz energy. The spectral transmission properties of all solid materials used in the THz beampath were measured using a ZnTe based optical rectification system[39] and a Michelson interferometer set-up. The total transmission of all materials in the THz beam path was measured by a far-infrared interferometer in combination with a hot Hg lamp and found to be 2.5×10^{-5}.

For $\theta_{\rm coll} = 30$ mrad, and electron beams containing up to 1.5 nC, the measured radiated energy per pulse between 0.3–2.9 THz was between 3–5 nJ/pulse.[10] For the set-up with collection angle covering 80-300 mrad

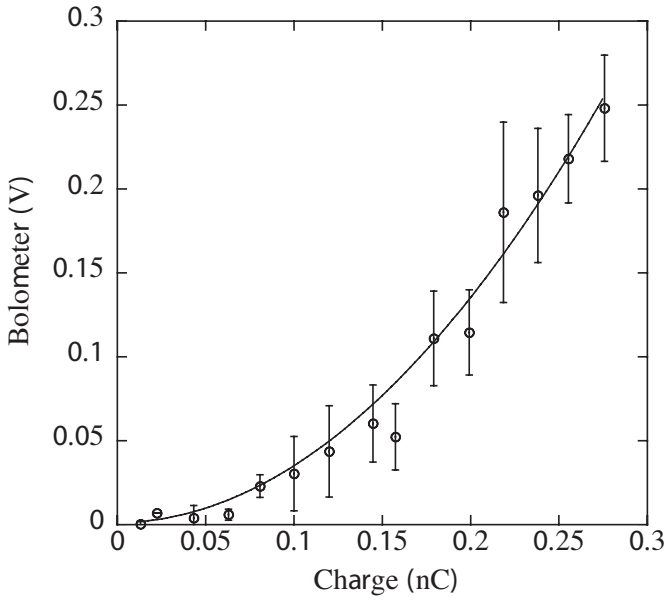

Figure 6. Bolometer voltage vs. charge per bunch for the 80-300 mrad collection half-angle. Each dot represents an average of 50 experimental shots, with rms variation as error bar. The solid line is a quadratic fit to the data, indicating coherence of the radiated signal. The bolometer (Infrared Laboratories) had a voltage responsivity $S = 2.73 \times 10^8$ V/W and thermal conductivity $G = 17.01$ μW/K. Since the radiation bursts are much shorter than the bolometer time constant, $\tau_{\rm bolo} = 0.33$ ms, the detector operates as a calorimeter. The absorbed energy is then given by: $E_{\rm absorbed} = G\tau_{\rm bolo}\Delta V_{\rm bolo}/(R\eta_{\rm bolo}) = 4.0 \times \Delta V_{\rm bolo}$ (in pJ), where $R = S \times G = 4.64$ is the induced voltage per K of temperature rise (in V/K), $\Delta V_{\rm bolo}$ is the height of the voltage pulse (in V), and $\eta_{\rm bolo} \sim 0.3$ is the bolometer efficiency. The radiated energy is $E_{\rm radiated} = E_{\rm absorbed}/\eta_{\rm coll}$, where $\eta_{\rm coll}$ is the overall collection efficiency of the system.

angles, the total radiated energy in the THz beam was approximately 70-80 nJ for electron bunches containing about 0.3 nC.

For the experimental parameters ($\rho = 100$ μm $\pm$ 15 μm, $\theta_{\rm coll} = 30$ mrad $^{+0\ \rm mrad}_{-10\ \rm mrad}$, 1.5 nC charge, and $u_{\rm T} m_e c^2$ = 4.6 MeV) the calculated energy per pulse is 2.3 nJ, which agrees within error bars with the 3–5 nJ measured experimentally. For the second case, using 0.3 nC charge, frequencies ranging from 0.3 to 19 THz, and angular coverage from 80-300 mrad, the calculated energy per pulse is on the order of 160 nJ, compared to 70-80 nJ experimentally. This is in reasonable agreement, given the sensitivity of the radiated energy to bunch length, plasma size, energy distribution and total charge.

To verify that the radiation is emitted coherently, the bunch charge was varied by changing either the laser pulse duration or the position of the gas jet with respect to the laser beam focal position.[16, 22] The dependence of the peak amplitude of the bolometer signal versus bunch charge is shown in Fig. 6. Radiation collected on the bolometer scales quadratic with charge consistent with coherent emission of radiation. We note here, that measurements carried out at 94 GHz also show quadratic dependence.[38]

5.2. Polarization Measurement

Since transition radiation is in principle radially polarized, a further test of the validity of our model was carried out by measuring the polarization characteristics of the source. A far-infrared wire-grid linear polarizer was placed at the entrance plane of the bolometer, where the THz radiation is brought to a focus. The polarizer angle was rotated from 0°–180° in steps of 30° and at each position about 30 shots were acquired. Within the error bars, the transmitted signal was found to be independent of the polarizer angle, consistent with radially polarized radiation.

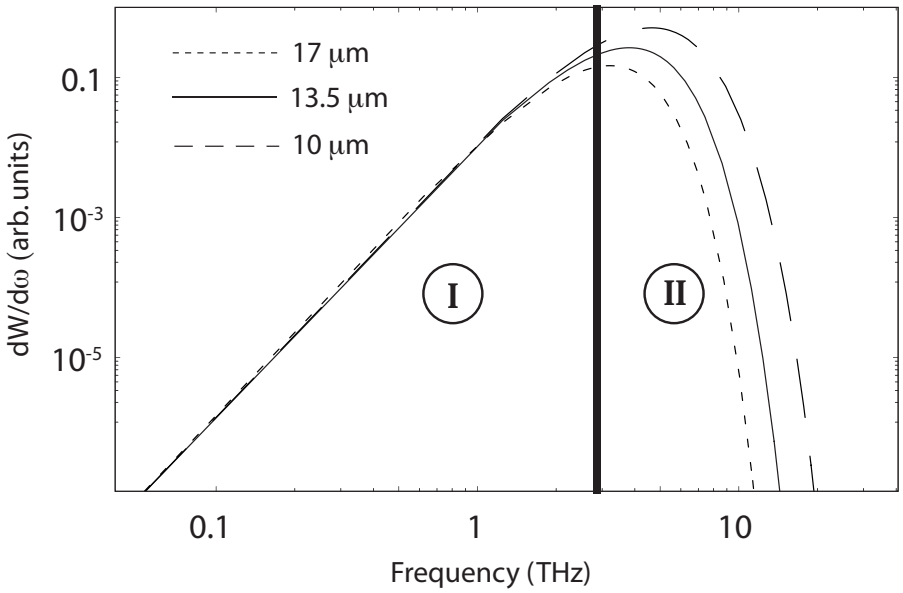

Figure 7. Calculated radiated energy vs. frequency within $80 < \theta_{coll} < 300$ mrad. The measured electron beam energy distribution was approximated using a Boltzmann distribution with a temperature of 4.6 MeV, the longitudinal electron beam distribution was assumed to be a Gaussian with 10, 13.5, and 17 μm rms length for the three curves shown, and the plasma to have a transverse half-width = 100 μm. The numbered spectral regions correspond to the two frequency ranges distinguished in the measurements by various filter combinations in the THz beam path.

5.3. Radiation Spectrum

As a first attempt to obtain spectral information of the THz source, the total radiated energy was collected in the 0.3–19 THz and in the 0.3–2.9 THz ranges (and hence 2.9–19 THz range). This was done with the use of two separate filters that were inserted between the bolometer window and the bolometer detector element. The first long pass filter consisted of a thin polyethylene filter with a diamond scattering layer, and had a cut-on wavelength of 16 μm (19 THz). The second long pass filter, made of crystal quartz with a broadband anti-reflection coating, had a cut-on wavelength of 103 μm (2.9 THz). Radiation at wavelengths longer than 1 mm (0.3 THz) was not detectable with the bolometer through its intrinsic design.

Analysis of the raw experimental data (averaging of several tens of shots) shows that 22% of the collected radiation was emitted in the frequency range 0.3 –2.9 THz, while 78% of the radiation was emitted within the frequency range 2.9–19 THz range. To model this data, the radiated spectrum was calculated including diffraction (see Sec. 2) from a 100 μm radius plasma column and again using a 4.6 MeV Boltzmann distribution for the electron bunch energy distribution. The spectrum of the radiation can be calculated assuming a longitudinal charge distribution and transverse size of the dielectric (plasma). Figure 7 shows spectra of the radiation for Gaussian longitudinal charge distributions with three different rms lengths: σ_z = 10, 13.5, and 17 μm transitioning out of a plasma with a transverse half-width of 100 μm. The short wavelength cut-off is due to the longitudinal coherence effects ($\lambda_{\min} \sim \sigma_z$), and the long wavelength cut-off is due to the influence of diffraction radiation from the transverse edge of the plasma ($\lambda_{\max} \sim \rho/u_{\mathrm{T}}$). The relative energy contents of the two spectral regions of the measurements (I. and II. in Fig. 7, corresponding to the frequency ranges of 0.3 to 2.9 THz and 2.9 to 19 THz, respectively) for the three modeled bunch lengths are 11%/89% for σ_z = 10.0 μm, 22%/78% for σ_z = 13.5 μm, and 37%/63% for σ_z = 17.0 μm. Comparing these numbers to the measured 22%/78% ratio, a deduction of σ_z = 13.5 μm for the electron bunch lengths at the plasma boundary seems reasonable. An rms bunch length on the order of 13 μm is also consistent with self-modulated LWFA simulations[40] which typically predict electron beam bunch lengths to be on the order of the laser pulse duration.

6. SUMMARY AND CONCLUSIONS

This work has presented theoretical and experimental results on the generation of transition radiation from laser accelerated electron bunches crossing a plasma-vacuum boundary. An LWFA produced fs duration electron bunches containing several nC of charge. Transition radiation at the plasma boundary occurs while the bunch is still very dense. This radiation is coherent and scales quadratically with charge for wavelengths long compared to the bunch length. The radiation is directed and intrinsically synchronized to the laser beam. The total radiated energy versus bunch charge was experimentally found to scale quadratically, consistent with a coherent emission process. The energy transmitted through a linearly polarizing wire grid was found to be independent on the rotation angle of the polarizer, consistent with radial polarization expected for transition radiation. Preliminary (coarse) spectral measurements were carried out using a set of long pass filters. The experimentally measured fraction of energy in the ranges 0.3–2.9 THz and 2.9–19 THz was 22% and 78%, respectively. The long and short wavelength spectral cut-off was shown to depend on the transverse plasma profile and bunch length, repectively. Good agreement with theory was obtained by assuming an electron bunch length ~ 13 μm and a plasma radius ~ 100 μm at the point where the radiation is produced. The bunch length would therefore be on the order of the laser pulse length, consistent with particle-in-cell code results.[40]

In the present experiment, 3–5 nJ-level pulses were collected within a limited 30 mrad collection angle,[10] and 70–80 nJ when collecting radiation in the angular range 80 – 300 mrad. For the latter case the charge per bunch was 0.3 nC. These measurements are in good agreement with predictions from theory. The measured THz pulse energy can be dramatically increased by a number of straightforward methods. Maximizing the amount of charge increases source performance, since the coherent transition radiation signal scales quadratically with bunch charge. Since the radiation is directed with an angular distribution which has a minimum on axis and an opening angle which is roughly $1/\gamma$ in the absence of diffraction effects but considerably larger for finite sized plasmas, increasing $\theta_{\rm coll}$ to 200 mrad, for the present experimental set-up, is expected to increase the collected energy per pulse to > 1 μJ for a bunch charge greater than 1 nC. Furthermore, 100 μJ/pulse could be achieved by increasing the transverse plasma size ρ to the mm-scale, thus minimizing diffractive effects.[14] This could be done by focusing a laser beam with cylindrical optics to produce a vertical mm-scale sheet-like plasma through which the electron beam propagates. Increasing the mean energy of the electron beam to the few 10's of MeV with, e.g., a channel-guided LWFA,[41] could further increase the pulse energy to the few 100 μJ level in a 0.1 rad cone. Such intense THz radiation will provide access to non-linear regimes and highly non-equilibrium processes using MV/cm field strengths and may also benefit single shot two-dimensional THz imaging. Improving the performance of laser driven accelerator will in turn be aided by the use of coherent emission of radiation at the plasma-vacuum boundary as a diagnostic tool, through its sensitivity to charge, energy distribution and bunch duration.

ACKNOWLEDGMENTS

The authors acknowledge contributions of B. Marcelis, D. Auerbach, D. Bruhwiler, B. Shadwick, L. Archambault, J. Byrd, M.C. Martin, J. Corlett, D. Li, M. Dickinson, S. DiMaggio, D. Syversrud, N. Ybarrolaza, J. Wallig, D. Calais, P. Catravas, F. Sannibale, J. Singley, M.A. Carnahan, R.A. Kaindl and D. Chemla. This work was supported by the U.S. Department of Energy under Contract No. DE-AC03-76SF0098. C.G.R. Geddes acknowledges the Hertz Foundation for support.

REFERENCES

1. D. M. Mittleman, M. Gupta, R. Neelamani, R. G. Baraniuk, J. V. Rudd, and M. Koch, "Recent advances in terahertz imaging," *Appl. Phys. B* **68**(6), pp. 1085–1094, 1999.
2. J. Orenstein and A. J. Millis, "Advances in the physics of high-temperature superconductivity," *Science* **288**(5465), pp. 468–474, 2000.
3. B. Ferguson, S. Wang, D. Gray, D. Abbot, and X.-C. Zhang, "T-ray computed tomography," *Opt. Lett.* **27**, pp. 1312–1314, 2002.
4. A. S. Weling, B. B. Hu, N. M. Froberg, and D. H. Auston, "Generation of tunable narrow-band THz radiation from large aperture photoconducting antennas," *Appl. Phys. Lett.* **64**, pp. 137–9, 1994.

5. X.-C. Zhang, B. B. Hu, J. T. Darrow, and D. H. Auston, "Generation of femtosecond electromagnetic pulses from semiconductor surfaces.," *Appl. Phys. Lett.* **56**(11), pp. 1011–13, 1990.
6. E. Budiarto, J. Margolies, S. Jeong, J. Son, and J. Bokor, "High intensity terahertz pulses at 1 kHz repetition rate," *IEEE J. Quantum Electron.* **32**(10), pp. 1839–46, 1996.
7. T. Nakazato, M. Oyamada, N. Niimura, S. Urasawa, O. Konno, A. Kagaya, R. Kato, T. Kamiyama, Y. Torizuka, T. Nanba, Y. Kondo, Y. Shibata, K. Ishi, T. Ohsaka, and M. Ikezawa, "Observation of coherent synchrotron radiation," *Phys. Rev. Lett.* **63**(12), pp. 1245–1248, 1989.
8. U. Happek, A. J. Sievers, and E. B. Blum, "Observation of coherent transition radiation," *Phys. Rev. Lett.* **67**, pp. 2962–2965, November 1991.
9. M. L. Ter-Mikaelian, *High-energy electromagnetic processes in condensed media*, Wiley-Interscience, New York, 1972.
10. W. P. Leemans, C. G. R. Geddes, J. Faure, C. Tóth, J. van Tilborg, C. B. Schroeder, E. Esarey, G. Fubiani, D. Auerbach, B. Marcelis, M. A. Carnahan, R. A. Kaindl, J. Byrd, and M. C. Martin, "Observation of THz emission from a laser-plasma accelerated electron bunch crossing a plasma-vacuum boundary," *Phys. Rev. Lett.* **91**, p. 074802, August 2003.
11. P. Kung, H. Lihn, H. Wiedemann, and D. Bocek, "Generation and measurement of 50-fs(rms) electron pulses," *Phys. Rev. Lett.* **73**(7), pp. 967–970, 1994.
12. W. D. Kimura, A. van Steenbergen, M. Babzien, I. Ben-Zvi, L. P. Campbell, D. B. Cline, C. E. Dilley, J. C. Gallardo, S. C. Gottschalk, P. He, K. P. Kusche, Y. Liu, R. H. Pantell, I. V. Pogorelsky, D. C. Quimby, J. Skaritka, L. C. Steinhauer, and V. Yakimenko, "First staging of two laser accelerators," *Phys, Rev, Lett.* **86**, pp. 4041–4043, 2001.
13. G. L. Carr, M. C. Martin, W. R. McKinney, K. Jordan, G. Neil, and G. P. Williams, "High-power terahertz radiation from relativistic electrons," *Nature* **420**(14), pp. 153–5, 2002.
14. C. B. Schroeder, E. Esarey, J. van Tilborg, and W. P. Leemans, "Theory of coherent transition radiation generated at a plasma-vacuum interface," *Phys. Rev. E* **69**, p. 016501, January 2004.
15. V. Malka, S. Fritzler, E. Lefebvre, M. M. Aleonard, F. Burgy, J. P. Chambaret, J. F. Chemin, K. Krushelnick, G. Malka, S. P. D. Mangles, Z. Najmudin, M. Pittman, J. P. Rousseau, J. N. Scheurer, B. Walton, and A. E. Dangor, "Electron acceleration by a wake field forced by an intense ultrashort laser pulse," *Science* **298**(5598), pp. 1596–1600, 2002.
16. W. P. Leemans, P. Catravas, E. Esarey, C. Geddes, C. Toth, R. Trines, C. B. Schroeder, B. A. Shadwick, J. van Tilborg, and J. Faure, "Electron-yield enhancement in a laser-wakefield accelerator driven by asymmetric laser pulses," *Phys. Rev. Lett.* **89**, p. 4802, 2002.
17. H. Hamster, A. Sullivan, S. Gordon, W. White, and R. Falcone, "Subpicosecond, electromagnetic pulses from intense laser-plasma interaction," *Phys. Rev. Lett.* **71**(17), pp. 2725–2728, 1993.
18. J. J. Santos, F. Amiranoff, S. D. Baton, L. Gremillet, M. Koenig, E. Martinolli, M. Rabec Le Gloahec, C. Rousseaux, D. Batani, A. Bernardinello, G. Greison, and T. Hall, "Fast electron transport in ultraintense laser pulse interaction with solid targets by rear-side self-radiation diagnostics," *Phys. Rev. Lett.* **89**, p. 025001, July 2002.
19. Y. Shibata, T. Takahashi, T. Kanai, K. Ishi, M. Ikezawa, J. Ohkuma, S. Okuda, and T. Okada, "Diagnostics of an electron beam of a linear accelerator using coherent transition radiation," *Phys. Rev. E* **50**, pp. 1479–1484, August 1994.
20. W. P. Leemans, C. W. Siders, E. Esarey, N. E. Andreev, G. Shvets, and W. B. Mori, "Plasma guiding and wakefield generation for second-generation experiments," *IEEE Trans. Plasma Sci.* **24**, pp. 331–342, 1996.
21. P. Volfbeyn, E. Esarey, and W. Leemans, "Guiding of laser pulses in plasma channels created by the ignitor-heater technique," *Phys. Plasmas* **6**, pp. 2269–2277, 1999.
22. W. P. Leemans, D. Rodgers, P. Catravas, C. Geddes, G. Fubiani, E. Esarey, B. Shadwick, R. Donahue, and A. Smith, "Gamma-neutron activation experiments using laser wakefield accelerators," *Phys. Plasmas* **8**, pp. 2510–2516, 2001.
23. C. Toth, J. Faure, J. van Tilborg, C. G. R. Geddes, C. B. Schroeder, E. Esarey, and W. P. Leemans, "Tuning of laser pulse shapes in grating-based compressors for optimal electron acceleration in plasmas," *Optics Letters* **28**(19), pp. 1823–1825, 2003.

24. E. Esarey, P. Sprangle, J. Krall, and A. Ting, "Overview of plasma-based accelerator concepts," *IEEE Trans. Plasma Sci.* **24**(2), pp. 252–288, 1996.
25. A. Modena, Z. Najmudin, A. E. Dangor, C. E. Clayton, K. A. Marsh, C. Joshi, V. Malka, C. B. Darrow, C. Danson, D. Neely, and F. N. Walsh, "Electron acceleration from the breaking of relativistic plasma waves," *Nature* **377**, pp. 606–608, 1995.
26. A. Ting, C. I. Moore, K. Krushelnick, C. Manka, E. Esarey, P. Sprangle, R. Hubbard, H. R. Burris, and M. Baine, "Plasma wakefield generation and electron acceleration in a self-modulated laser wakefield accelerator experiment," *Phys. Plasmas* **4**, p. 1889, 1997.
27. C. Gahn, G. D. Tsakiris, A. Pukhov, J. Meyer-ter-Vehn, G. Pretzler, P. Thirolf, D. Habs, and K. J. Witte, "Multi-MeV electron beam generation by direct laser acceleration in high-density plasma channels," *Phys. Rev. Lett.* **83**, pp. 4772–4775, December 1999.
28. X. Wang, M. Krishnan, N. Saleh, H. Wang, and D. Umstadter, "Electron acceleration and the propagation of ultrashort high-intensity laser pulses in plasmas," *Phys. Rev. Lett.* **84**, pp. 5324–5327, June 2000.
29. M. I. K. Santala, Z. Najmudin, E. L. Clark, M. Tatarakis, K. Krushelnick, A. E. Dangor, V. Malka, J. Faure, R. Allott, and R. J. Clarke, "Observation of a hot high-current electron beam from a self-modulated laser wakefield accelerator," *Phys. Rev. Lett.* **86**(7), pp. 1227–1230, 2001.
30. K. Krushelnick (private communication, 2003).
31. M. I. K. Santala, M. Zepf, F. N. Beg, E. L. Clark, A. E. Dangor, K. Krushelnick, M. Tatarakis, I. Watts, K. W. D. Ledingham, T. McCanny, I. Spencer, A. C. Machacek, R. Allott, R. Clarke, and P. A. Norreys, "Production of radioactive nuclides by energetic protons generated from intense laser-plasma interactions," *Appl. Phys. Lett.* **78**(1), pp. 19–21, 2001.
32. G. Dugan, A.Misuri, and W. P. Leemans, "Design and performance estimates for the l'OASIS experiment magnetic spectrometers," Tech. Rep. LBNL-49394, Lawrence Berkeley National Laboratory, December 2001.
33. T. Hosokai, K. Kinoshita, A. Zhidkov, K. Nakamura, T. Watanabe, T. Ueda, H. Kotaki, M. Kando, K. Nakajima, and M. Uesaka, "Effect of a laser prepulse on a narrow-cone ejection of MeV electrons from a gas jet irradiated by an ultrashort laser pulse," *Phys. Rev. E* **67**, p. 036407, March 2003.
34. S.-Y. Chen, M. Krishnan, A. Maksimchuk, R. Wagner, and D. Umstadter, "Detailed dynamics of electron beams self-trapped and accelerated in a self-modulated laser wakefield," *Phys. Plasmas* **6**, pp. 4739–4749, December 1999.
35. A. W. Chao, R. Pitthan, T. Tajima, and D. Yeremian, "Space charge dynamics of bright electron beams," *Phys. Rev. ST Accel. Beams* **6**, p. 024201, February 2003.
36. G. Fubiani, G. Dugan, W. Leemans, E. Esarey, and J. L. Bobin, "Semi-analytical 6d space charge model for dense electron bunches with large energy spreads," in *Proc. of the 2002 Advanced Accelerator Concepts Workshop*, C. E. Clayton and P. Muggli, eds., **647**, pp. 203–212, AIP, (NY), 2002.
37. S. Fritzler (private communication, 2003).
38. W. P. Leemans, J. van Tilborg, J. Faure, C. G. R. Geddes, C. Tóth, C. B. Schroeder, E. Esarey, G. Fubiani, and G. Dugan, "Terahertz radiation from laser accelerated electron bunches," *Phys. Plasmas* **11**, 2004. in press.
39. D. Grischkowsky, S. Keiding, M. van Exter, and C. Fattinger, "Far-infrared time-domain spectroscopy with terahertz beams of dielectrics and semiconductors," *J. Opt. Soc. Am. B* **7**, pp. 2006–2015, 1990.
40. K. C. Tzeng, W. B. Mori, and T. Katsouleas, "Electron beam characteristics from laser-driven wave breaking," *Phys. Rev. Lett.* **79**(26), pp. 5258–61, 1997.
41. A. J. W. Reitsma, W. P. Leemans, E. Esarey, C. B. Schroeder, L. P. J. Kamp, and T. J. Schep, "Simulation of electron postacceleration in a two-stage laser wakefield accelerator," *Phys. Rev. ST Accel. Beams* **5**(5), p. 051301, 2002.